

Family of boron fullerenes: general constructing schemes, electron counting rule and *ab initio* calculations

Qing-Bo Yan, Xian-Lei Sheng, Qing-Rong Zheng, Li-Zhi Zhang, Gang Su*

College of Physical Sciences, Graduate University of Chinese Academy of Sciences, P. O. Box 4588, Beijing 100049, China

A set of general constructing schemes are unveiled to predict a large family of stable boron monoelemental, hollow fullerenes with magic numbers $32+8k$ ($k \geq 0$). The remarkable stabilities of these new boron fullerenes are then studied by intense *ab initio* calculations. An electron counting rule as well as an isolated hollow rule are proposed to readily show the high stability and the electronic bonding property, which are also revealed applicable to a number of newly predicted boron sheets and nanotubes.

PACS numbers: 81.05.Tp, 61.48.+c, 81.07.Nb, 82.20.Wt

Carbon nanostructures such as fullerenes, nanotubes and graphenes [2, 3, 4, 5] have been extensively studied in the past decades. As boron and carbon are neighbors in the periodic table, and possess many structural analogies [6, 7], it is expected that boron could also form nanostructures similar to carbon. The boron clusters, nanotubes (BNT) and sheets are thus actively explored in recent years [8, 9, 10]. More currently, a stable boron fullerene B_{80} was predicted [11], and a new type of boron sheet (NBS) and related BNTs [12, 13] were found to be remarkably more stable than the boron sheet and BNTs with triangular structures; several other fullerene-like boron nanostructures are also predicted [14, 15]. In this Letter, we shall present generic constructing schemes that can produce a large family of novel stable boron nanostructures that include B_{80} buckyball and the NBS as members.

Let us start with analyzing the geometrical structures of B_{80} and the NBS. They contain three basic motifs: hollow pentagon (HP), hollow hexagon (HH), and filled hexagon (FH) (i.e. hexagon with an additional atom in center), respectively. A closer inspection reveals that both B_{80} and NBS are entirely composed of such a snowdrop-like structure [Fig. 1(a)] in that a central FH is surrounded by three FHs and three "hollows" (HPs or HHs), and every FH can be viewed as the center of the structure. For B_{80} and the NBS, the HPs and HHs act as "hollows", respectively [Figs. 1(b) and (c)]. In light of this observation, we shall show that such a snowdrop-like structure plays a critical role in the stability of B_{80} and NBS as well as other boron quasi-planar structures (fullerenes, sheets, nanotubes, etc), and thus can be utilized as building blocks to construct novel boron nanostructures. Henceforth, the boron fullerenes that are composed of snowdrop-like structures are coined as S-fullerenes for brevity.

Geometrically, in an S-fullerene, every HP should be surrounded by five FHs, and every HH is surrounded by six FHs, whereas there are three "hollows" (HPs or HHs) around every FH. Thus we have $5N_{HP} + 6N_{HH} = 3N_{FH}$, where N_{HP} , N_{HH} , and N_{FH} denote the number of HP, HH, and FH, respectively. If we take the S-fullerene as a polyhedron, and each HP, HH or FH as a surface, then Euler theorem, e (edges) + 2 = v (vertices) + f (faces), leads to $N_{FH} = 12$, implying that in an S-fullerene the number of hollow pentagons should be exactly 12. Consequently, we have $N_{FH} = 20 + 2N_{HH}$.

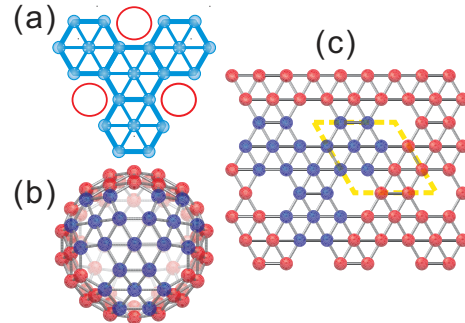


FIG. 1: (Color online) The snowdrop-like structures in B_{80} and new boron sheet (NBS). (a) a snowdrop-like motif, in which a filled hexagon (FH) is surrounded by three FHs and three "hollows" (pentagons or hexagons, denoted by circles); (b) B_{80} ; (c) NBS, the yellow parallelogram indicates an unit cell of the NBS. The blue atoms form the snowdrop-like units in B_{80} and NBS.

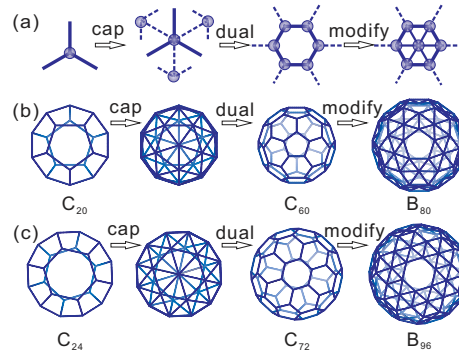


FIG. 2: (Color online) Illustration of leapfrog and modified leapfrog transformations. (a) a three-connected vertex becomes a new hexagon (in leapfrog) or a hexagon with an additional atom in center (in modified leapfrog); (b) a C_{20} converts to C_{60} and B_{80} by the leapfrog and modified leapfrog transformations, respectively; (c) a C_{24} transforms to C_{72} and B_{96} .

In an S-fullerene the total number of boron atoms should be $n = [5N_{HP} + 6(N_{HH} + N_{FH})]/3 + N_{FH} = 80 + 8N_{HH}$. For B_{80} , since $N_{HH} = 0$, $N_{FH} = 20$, and $n = 80$.

These relations put restrictions in searching for S-fullerenes, but they are still inadequate to find the concrete geometrical structures. Fortunately, through intensive attempts

we disclose that a modified leapfrog transformation (MLT) is useful to generate S-fullerenes. The original leapfrog transformation [16] has been applied to construct the so-called electronic closed-shell fullerenes C_{60+6k} (leapfrog-fullerenes). To produce S-fullerenes, the only thing we should do is to modify the operations shown in Fig. 2(a). In the original leapfrog operations, every vertex transforms to an HH (containing six atoms). Here we propose an MLT, in which every vertex converts to an FH (containing seven atoms), suggesting that every vertex of the original polyhedron provides an extra atom. Since these extra atoms could compose a polyhedron identical to the original one, the MLT can be considered as the combination of the original polyhedron and its leapfrog. For instance, B_{80} , the modified leapfrog of C_{20} , could be viewed as a combination of C_{20} and its leapfrog C_{60} structures [Fig. 2(b)]. As a result, in the final modified leapfrog structure, the number of atoms grows four times vertices as many as the original, i.e., $80 + 8k$ ($k \geq 0, k \neq 1$), while the symmetry is still kept. The most important point is that all structures generated by the MLT fall into the S-fullerenes. Through a reverse transformation, every S-fullerene could be converted to the original polyhedron. Therefore, B_{80+8k} ($k \geq 0, k \neq 1$) can be produced from the structure of C_{20+2k} ($k \geq 0, k \neq 1$) by means of the MLT [Figs. 2 (b) and (c)]. The isomer numbers of both C_{60+6k} and B_{80+8k} are equal to that of C_{20+2k} for each k ($k \geq 0, k \neq 1$), and the numbers of valence electrons are identical for C_{60+6k} and B_{80+8k} with the same k . In addition, the MLT may also be applied to generate other quasi-planar structures composed of snowdrop-like units. As the leapfrog of a graphene structure is still graphene, the MLT of graphene leads to the NBS structure; similarly, the structures of BNTs can be generated by the MLT of CNTs.

Several structures of boron S-fullerenes as examples shown in Fig. 3 have been generated and then studied by means of *ab initio* calculations [17]. The isomer numbers and symmetries of B_{80+8k} are listed in Table I. For $k = 6, 7, 8, 9, 10, \dots$, the isomer number is 6, 6, 15, 17, 40..., respectively, which grows rapidly with increasing k . For instance, when $k = 0$, the corresponding S-fullerene is the known spherical B_{80} [11]; when $k = 2$, it produces B_{96} [Fig. 3(a)], which bears D_{6d} symmetry and has a round pillow shape with two HHs located at the D_{6d} axis; when $k = 3$, it gives a pineapple shaped B_{104} with D_{3h} symmetry [Fig. 3(b)]; when $k = 4$, it generates B_{112} [Figs. 3(c)-(d)], which has two isomers: one possesses D_2 symmetry with an elliptical pillow shape, while another has T_d symmetry and looks like a regular tetrahedron with four smoothed vertices; when $k = 5$, it yields B_{120} [Figs. 3(e)-(g)], which has three isomers with one bearing D_{5h} symmetry, and the other two having C_{2v} symmetry. The D_{5h} B_{120} has a cylinder capsule shape, and can be viewed as a short open-end BNT B_{40} unit (which is rolled from NBS) capped with two halves of B_{80} . This capped BNT can be elongated by repeating the middle open-end BNT B_{40} unit to generate similar D_{5h} symmetry capped BNTs B_{80+40t} ($t \geq 1$) [14, 18], all of which belong to a subset of B_{80+8k} . Generally, using a proper S-fullerene as the cap, and the open-end BNT with different

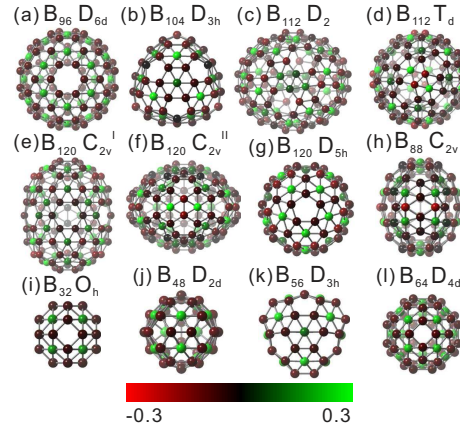


FIG. 3: (Color online) Schematic structures and Mulliken atomic charge populations of several boron S-fullerenes. The unit of color bar is electrons.

TABLE I: The number (N_{iso}), symmetries, relative energies per atom (E , in eV, relative to that of graphene and NBS, respectively), and HOMO-LUMO gap energies (ΔE , in eV) of C_{60+6k} and S-fullerenes B_{80+8k} ($k \leq 5$) isomers (obtained with Gaussian03).

k	N_{iso}	symmetry	$C_{n=60+6k}$			$B_{n=80+8k}$				
			n	E	ΔE	n	E	ΔE	N_{HH}	
0	1	I_h	60	0.386	1.670	80	0.179	1.020	0	20
1	0	-	-	-	-	-	-	-	-	-
2	1	D_{6d}	72	0.365	1.445	96	0.160	0.784	2	24
3	1	D_{3h}	78	0.346	1.460	104	0.151	0.738	3	26
4	2	D_2	84	0.339	1.367	112	0.146	0.682	4	28
		T_d	84	0.329	1.632	112	0.141	0.927	4	28
5	3	C_{2v}^I	90	0.321	1.364	120	0.137	0.709	5	30
		C_{2v}^{II}	90	0.322	1.489	120	0.136	0.828	5	30
		D_{5h}	90	0.312	1.029	120	0.135	0.555	5	30

sizes as the body, the other similar subsets of boron nanotubes could be generated.

The energies of C_{60+6k} and B_{80+8k} ($k \neq 1, k \leq 5$) relative to graphene and NBS, respectively, are listed in Table I. Note that different isomers with the same k may have different structures and symmetries. It can be seen that the relative energies decrease with the increase of k for both C_{60+6k} and B_{80+8k} , which are expected to converge to the values of graphene [16] and NBS, respectively, suggesting that the stabilities of both fullerenes increase with the growth of size. Thus, B_{80+8k} ($k \geq 0, k \neq 1$) gives rise to a large class of stable boron fullerenes, where B_{80} is just the first member of this family, while the NBS is the infinite k analogue. To check further the stabilities of these boron fullerenes, we calculate the total energies per atom for the caged B_{80+8k} ($k \neq 1, k \leq 5$) with other different structures that do not belong to the S-fullerene family, and find that they are all less stable than those of S-fullerenes. Note that B_{96} is about 0.019 eV/atom more stable than B_{80} in energy, and the members with larger k have even more lower relative energies. The present class of S-fullerenes are more stable than B_{180} proposed earlier [14].

In the preceding S-fullerenes, only are HP and HH con-

sidered as boron "hollows". If we take the hollow quadrangle (HQ) into account, then the S-fullerenes would be extended. For the boron fullerenes composed of HQ, HP, HH, and FH, the total number of boron atoms satisfies $n = [4N_{HQ} + 5N_{HP} + 6(N_{HH} + N_{FH})]/3 + N_{FH}$, while Euler theorem requires $N_{HP} + 2N_{HQ} = 12$, and $N_{FH} = 20 + 2(N_{HH} - N_{HQ})$. Then, we have $n = 80 + 8(N_{HH} - N_{HQ})$. Consider a few special cases. (a) If $N_{HQ} = 0$, it recovers to the preceding B_{80+8k} ($k \geq 0, k \neq 1$); (b) If $N_{HP} = 0$, we get $N_{HQ} = 6$, $N_{FH} = 8 + 2N_{HH}$, and $n = 32 + 8N_{HH}$, which leads to B_{32+8k} ($k \geq 0$) that consist of HQs, HHs and FHs; (c) If $N_{HH} = 0$, we have $N_{FH} = 20 - 2N_{HQ}$, $n = 80 - 8N_{HQ}$, and $0 < N_{HQ} \leq 6$, which corresponds to B_{32+8k} ($0 \leq k < 6$) that are composed of HQs, HPs and FHs. As examples, O_h B_{32} , D_{5h} B_{40} , D_{2d} B_{48} , D_{3h} B_{56} , D_{4d} B_{64} , and D_{3h} B_{72} can be obtained, as shown in Figs. 3(i)-(l); (d) If $N_{HH} - N_{HQ} = 1$, then B_{88} can be formed, which has abundant isomers because N_{HH} and N_{HQ} can have various combinations to satisfy such a difference of unity. The structure of one C_{2v} B_{88} isomer is given in Fig. 3(h). *Ab initio* calculations show that these several isomers also follow the trend that relative energies per boron atom decrease with the increase of k . Thus if quadrangles were added to the set of "hollows", we would have a class of fullerenes B_{32+8k} ($k \geq 0$), and their isomers also increase largely for every k , which can be generated by the MLT as well, and enriches the family of boron fullerenes.

By carefully checking the structures of the S-fullerenes and NBS, we uncover an electron counting rule (ECR) and an isolated hollow rule (IHR) that would manifest the fundamental importance of the snowdrop-like structure and, reasonably explain the high stability and reveal the electronic bonding property of these boron nanostructures. Let us look again at the structures of B_{80} and NBS. The former is composed of 12 HPs and 20 FHs, while a unit cell of NBS has one HH and two FH [Fig. 1(c)]. As one FH can be viewed as a group of six triangles, B_{80} contains 120 triangles and an NBS unit cell has 12 triangles. Since each boron atom has three valence electrons, one may find that the total number of valence electrons of B_{80} is 240, just twice the number of triangles. Interestingly, the NBS has the same electron counting feature, as one unit cell has 8 boron atoms, contributing 24 valence electrons, which is just also twice the number of triangles it possesses. It is easy to substantiate that all of the S-fullerenes follow this electron counting scheme. In the central FH of a boron snowdrop-like unit, the atoms on six periphery vertices are shared by the neighboring FHs, and only is the central atom monopolized, so the net number of boron atoms that the central FH has is only four, and the corresponding number of valence electrons is 12, just twice the six triangles it possesses. Since all FHs in the S-fullerenes can be viewed as the central FHs of snowdrop-like structures, being equivalent to the above electron counting scheme, the total number of valence electrons of S-fullerenes are twice the number of triangles they have.

Such an agreement on electron counting property is not ac-

idental, which could be rationalized in a simple way [19]. As is well-known, the multi-center deficient-electron bonding scheme exists widely in boron structures [20]. Suppose that three boron atoms on the vertices of a triangle share a three-center two-electron bond, i.e., a triangle would consume two electrons, then the above ECR could be properly understood in a way that, in stable quasi-planar boron structures that are composed of FHs, HPs and HHs, etc., the total number of the valence electrons is equal to twice the number of triangles they contain, leading to that the number of boron atoms is as quadruple as the number of FHs ($n = 4N_{FH}$). The ECR is thus consistent with the snowdrop-like structure, as the latter is a kind of the geometrical realization of ECR, whilst the ECR can be considered as the electronic interpretation of the snowdrop-like unit. On the other hand, in all S-fullerenes, the "hollows" (HPs and HHs) are separated by FHs, as the requirement that every FH should be the center of a snowdrop-like structure cannot be satisfied if there exist any adjacent "hollows". Therefore, an IHR for boron S-fullerenes can be expected. The leapfrog procedure never generates adjacent pentagons [16], and similarly, the MLT never produces adjacent "hollows". It is interesting to note that the NBS and the related BNTs also follow the ECR and IHR, which suggests that the above two rules may be applicable to other boron nanostructures. While the IHR calls for boron "hollow" be well-separated by FHs, the ECR requires a quantitative constraint between the number of boron "hollows" and that of FHs. Consequently, the IHR and ECR are mutually constrained, which results in appropriate boron nanostructures.

The electronic structures of B_{80+8k} are obtained by the *ab initio* calculations. Figure 3 shows the Mulliken atomic charge populations of several S-fullerenes. The boron atoms in centers of FHs are marked in green, showing they are positively charged, while most of others are red, indicating they are negatively charged. Recall that all carbon atoms in C_{60+6k} are electroneutral. With regard to electron transfers in B_{80+8k} , the central atoms of FHs act as electron donors, and the other atoms act as electron acceptors, which are consistent with the donor-acceptor hypothesis on NBS [12], and also the charge transfer in monoatomic systems [21].

The gap energies between the lowest-unoccupied-molecular-orbital (LUMO) and the highest-occupied-molecular-orbital (HOMO) of C_{60+6k} and B_{80+8k} ($0 \leq k \leq 5, k \neq 1$) are listed in Table I. Interestingly, the isomers of both fullerenes with $k = 0$ (I_h), 4 (T_d), 5 (C_{2v}^{II}) have larger gap energies than their near neighbors. Fig. 4(a) shows the energy levels around the HOMO-LUMO gaps of C_{60+6k} and B_{80+8k} ($k = 0, 2, 3$). For the major energy levels of B_{80+8k} , one may find correspondences to their C_{60+6k} counterparts with the same degeneracy and symmetry. For instance, C_{60} and B_{80} both have a five-fold degenerate h_u HOMO and a three-fold degenerate t_{1u} LUMO [22]; C_{72} and B_{96} , C_{78} and B_{104} also exhibit similar corresponding relations as indicated in Fig. 4(a). The visualizations of the HOMO and LUMO of B_{80+8k} ($k = 0, 2, 3$) are presented in Figs. 4(b)-(d). We find the main profiles of corresponding

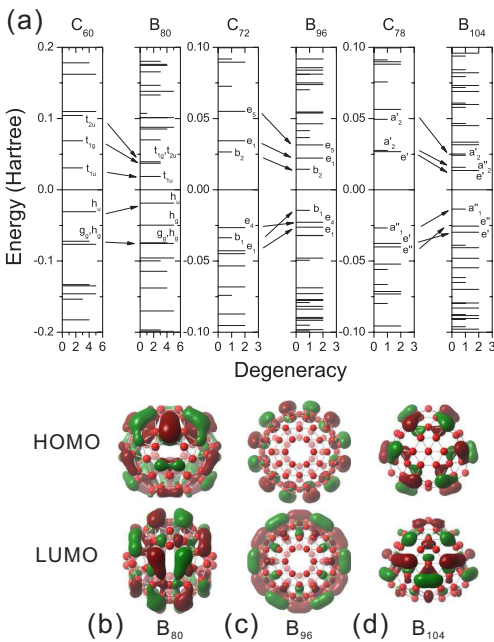


FIG. 4: (Color online) (a) Energy levels near HOMO-LUMO gaps of C_{60} , B_{80} , C_{72} , B_{96} , C_{78} , and B_{104} ; The profiles of HOMO and LUMO orbitals of (b) B_{80} ; (c) B_{96} and (d) B_{104} .

MOs (C_{60+6k} MOs are not shown here) exhibit striking similarity between C_{60} and B_{80} , C_{72} and B_{96} , C_{78} and B_{104} , and so forth. We believe that such an observation from the first several members of B_{80+8k} family would be kept for the members with even larger k . Since the frontier MOs dominate the primary chemical property of a molecule, B_{80+8k} may have chemical properties similar to the corresponding C_{60+6k} . Besides, as the carbon fullerenes can be stabilized by the exohedral chemical deriving and metallic endohedral method [23, 24, 25], the stability of boron fullerenes might also be improved in the same manner.

In summary, the general constructing schemes were proposed to construct a large family of stable boron fullerenes, whose remarkable stabilities were confirmed by intensive first-principles simulations. The empirical ECR and IHR were suggested to readily explain the geometrical stability and reveal the electronic bonding of the predicted boron fullerenes, which can also be shown applicable to boron quasi-planar structures such as nanotubes and sheets, and be useful for seeking for other stable boron nanostructures. The present predictions are awaited to synthesize experimentally, which may bring about a new dimension of boron chemistry.

All of the calculations are completed on the supercomputer NOVASCALe 6800 in Virtual Laboratory of Computational Chemistry, Supercomputing Center of Chinese Academy of Sciences. This work is supported in part by the National Science Foundation of China (Grant No. 10625419).

- [2] H. W. Kroto, J. R. Heath, S. C. O'Brien, R. F. Curl, R. E. Smalley, *Nature* **318**, 162 (1985).

[3] P. W. Fowler, D. E. Manolopoulos, *An Atlas of Fullerenes* (Clarendon Press, Oxford, 1995).

[4] R. Saito, G. Dresselhaus, and M. S. Dresselhaus, *Physical Properties of Carbon Nanotubes* (Imperial College Press, London, 1998).

[5] A. K. Geim, K. S. Novoselov, *Nature Mater.* **6**, 183 (2007).

[6] E. D. Jemmis, E. G. Jayasree, *Acc. Chem. Res.* **36**, 816 (2003).

[7] H. J. Zhai, B. Kiran, J. Li, L. S. Wang, *Nature Mater.* **2**, 827 (2003).

[8] I. Boustani, *J. Solid State Chem.* **133**, 182 (1997); *Surf. Sci.* **370**, 355 (1997); I. Boustani *et al.*, *J. Chem. Phys.* **110**, 3176 (1999); *Europhys. Lett.* **39**, 527 (1997); *Chem. Phys. Lett.* **311**, 21 (1999).

[9] M. H. Evans, J. D. Joannopoulos, S. T. Pantelides, *Phys. Rev. B* **72**, 045434 (2005).

[10] J. Kunstmann, A. Quandt, *Phys. Rev. B* **74**, 035413 (2005).

[11] N. G. Szwacki, A. Sadrzadeh, and B. I. Yakobson, *Phys. Rev. Lett.* **98**, 166804 (2007).

[12] H. Tang, S. Ismail-Beigi, *Phys. Rev. Lett.* **99**, 115501 (2007).

[13] X. Yang, Y. Ding, J. Ni, *Phys. Rev. B* **77**, 041402(R) (2008).

[14] N. G. Szwacki, *Nanoscale Res. Lett.* **3**, 49 (2008).

[15] D. L. Prasad and E. D. Jemmis, *Phys. Rev. Lett.* **100**, 165504 (2008).

[16] P. W. Fowler, *Chem. Phys. Lett.* **131**, 444 (1986); *J. Chem. Soc. Faraday Trans.* **86**, 2073 (1990); P. W. Fowler *et al.*, *J. Chem. Soc. Commun.* 1403 (1987).

[17] All of calculations were performed using Gaussian 03 [26] with PBEPBE density functional [27] and all-electron 6-31G(d, p) basis set [28] employed. The geometrical structures are optimized until the total energy and force achieve the tolerance of about 1×10^{-8} Hartree and 4.5×10^{-4} Hartree Bohr, respectively. The relative energies and HOMO-LUMO gaps were rechecked by using Quantum-ESPRESSO package [29] with ultrasoft Vanderbilt pseudopotentials [30] and generalized gradient corrected exchange and correlation functional PBE [27] employed. The results agree quite well.

[18] A. K. Singh, A. Sadrzadeh, and B. I. Yakobson, *Nano Letters* **8**, 1314 (2008).

[19] Q.-B. Yan, Q.-R. Zheng, and G. Su, *Phys. Rev. B* **77**, 224106 (2008).

[20] W. N. Lipscomb, *Acc. Chem. Rec.* **6**, 257 (1973).

[21] J. He, E. Wu, H. Wang, R. Liu, and Y. Tian, *Phys. Rev. Lett.* **94**, 015504 (2005).

[22] G. Gopakumar, M. T. Nguyen, and A. Ceulemans, *Chem. Phys. Lett.* **450**, 175 (2008).

[23] S. Xie, F. Gao, X. Lu, R. Huang *et al.*, *Science* **304**, 699 (2004).

[24] C. Wang, Z. Shi, L. Wan *et al.*, *J. Am. Chem. Soc.* **128**, 6605 (2006).

[25] Q.-B. Yan, Q.-R. Zheng, and G. Su, *J. Phys. Chem. C* **111**, 549 (2007).

[26] M. J. Frisch *et al.*, *Gaussian 03* (Gaussian, Inc., Wallingford CT, 2004).

[27] J. P. Perdew, K. Burke, M. Ernzerhof, *Phys. Rev. Lett.* **77**, 3865 (1996).

[28] P. C. Hariharan, J. A. Pople, *Theor. Chim. Acta* **28**, 213 (1973).

[29] P. Giannozzi *et al.*, *Quantum-espresso* (<http://www.pwscf.org>).

[30] D. Vanderbilt, *Phys. Rev. B* **41**, 7892 (1990).

[1] *Corresponding author. Email: gsu@gucas.ac.cn